ICEUBI2013 University of Beira Interior Faculty of Engineering Covilhã | Portugal
November 27 28 29 International Conference on Engineering Engineering for Economic Development

Control Systems for UAV Flight Testing

Joaquim Sousa, Pedro Santos, Pedro Gamboa
Department of Aerospace Sciences, Faculty of Engineering, University of Beira Interior, Covilhã, Portugal
joaquimsousa91@sapo.pt, p_daniel_santos@hotmail.com, pgamboa@ubi.pt

Conference Topic – CT 02

Abstract

This paper describes the work done on the instrumentation and flight testing of a fully autonomous UAV. This UAV, called Olharapo, has two configurations, one being fitted with a conventional fixed wing and the other fitted with a variable-span morphing wing. The main goal of this work is to characterize the flight performance of the UAV on the two configurations in order to establish a comparison between these two wings. For that purpose, an off-the-shelf UAV, the Skywalker with 1880mm wing span, is fitted with the same systems that are going to be installed on the Olharapo UAV. The objective of installing these systems on the Skywalker UAV is to safely measure the performance and validate all the systems in flight. This paper describes the work done regarding instrumentation, development of flight testing procedures and flight testing the Skywalker UAV.

Key Words: UAV, Autopilot, FPV, Morphing Wing

1. Introduction

In the past years the development of morphing wing technologies has been a matter of great interest from the scientific community. These technologies have in view the operation of an aircraft on its near-optimal performance point by means of wing geometric transformation. It has been demonstrated by Tidwell et al [1] that morphing wing technologies contributes for efficient performance during distinct mission roles, or enable new multi-role missions that are not possible with a fixed geometry aircraft.
There are several works developed around methods of wing morphing. These methods can be categorized into: planform alterations that include span [2,3,4], sweep [3] and chord; out-of-plane transformation such as twist [5], dihedral and span-wise bending; and airfoil adjustment regarding camber [6] and thickness. Focusing now on wing span variation, many different concepts have been tested. For example, from the pneumatic telescopic spars by Blondeau *et al* [7], the honeycomb structure with elastomer skin actuated by a pneumatic artificial muscle by Robert D. Vocke et al [4] to the telescopic wing servo/pulley-actuated by Vale *et al* [8] among many others. Other concepts are more radical and involve more than one type of wing transformation such as the fully adaptive model with seven degrees of freedom developed by Neal et al [3] or the completely different concept developed by NextGen, the batwing morphing, that was already flight tested after extensive design and wind tunnel testing [9,10]. Many other projects have been done on aircraft morphing concepts with the goal of enhancing performance and increasing energy efficiency of aircraft [10]. As a recent technology, the development of a morphing aircraft is an iterative process between design and experiment and extensive work as been done regarding aerodynamic shape optimization of airfoils and wings and multidisciplinary design optimization of wing systems [3,12,13,14,15].
The use of unmanned air vehicles (UAVs) as a platform for testing morphing wing concepts as a great potential, because UAVs can perform tasks considered dangerous without putting the crew in risk. Moreover they have much lower development and production costs and do not need the same infrastructures for operating when compared to manned aircraft.
In order to characterize the flight dynamics of an aircraft, it is required that the aircraft is well instrumented with sensors that give all the necessary data to perform a flight dynamics analysis. In this matter, some works have been performed that compare the calculated flight dynamics to the experimental flight dynamics [15].
The work described in this paper is about instrumentation and flight testing the Skywalker UAV so that all the systems involved for determining the performance of the aircraft Olharapo can safely be validated. The Olharapo UAV was developed at University of Beira Interior and has two configurations: one uses a fixed wing and the other is fitted with a variable-span

morphing wing.

2. First Person View System

In order to perform long range flights without line of sight, a first person view (FPV) system is required. This is very useful for data acquisition as it will be explained later in the current work. The FPV system is constituted by two major assemblies: the ground control station (GCS) and the airborne components.

2.1 The ground control station

The main function of the FPV GCS is to allow the pilot to see the real time video feed of the UAV, as if he were on a real cockpit. The components of the assembly are a 1.3GHz analog video receiver, a 12.1" LCD screen, a digital video recorder that records all flight videos to a memory card, two battery voltage checkers, a power module that distributes the power to all the ground station equipment and contains a video buffer that ensures a clean video signal to all connected devices and finally two Lithium-Ion polymer (Lipo) batteries that power all the ground station equipment.
The video receiver is connected to either a skew planar wheel or a heliaxial high directivity (11dBi) antenna. The former one is used when long range is desirable and the other for close range flights (less than 3km). The video display screen is a high brightness 12.1" LCD that has the particularity of not having a bluescreen when the signal strength is week. This is of utmost importance because in the eventuality of video signal degradation, the monitor will continue to show the noisy video feed. The two Lipo battery power sources are able to provide power for more than 12 hours of continuous operation. The control ground station is shown in Figure 1 with two different video receiver antennas.

(a) (b)

Figure 1- Complete ground control station showing the video receiver connected to: a) skew planar wheel antenna and b) heliaxial high directivity antenna.

2.2 The airborne components

The main airborne components are a video camera with pan and tilt motion, a microphone, an On-screen Display (OSD) that overlaps all the relevant data for piloting purposes on the video signal before being broadcasted, and a transmitter that feeds the video signal to the GCS. All the referred components are assembled in a detachable pod to allow an easy and fast installation and also to allow easy access to the fuselage interior.
The airborne components are powered up using the balance charge plug of the flight battery. In order to avoid noise coming from the brushless motor on the video signal, an LC filter is

used in series with the flight battery. The pan and tilt support is made of laser cut plywood and is actuated by two micro servos that are responsible for the pan and tilt motion. The video transmitter has 600mW of radiated power and is equipped with a skew planar wheel which is a low directivity circular polarized antenna. All the FPV antennas use circular polarized antennas since they have two distinct advantages: multipath interference is rejected, and polarization is not lost when the aircraft is banked during a turn. The airborne FPV system components are shown in Figure 2 fitted to the Skywalker UAV.

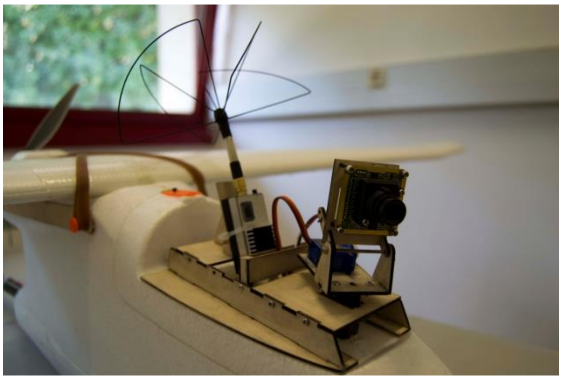

Figure 2-Detachable pod carrying the airborne FPV system components

3. Long range radio control system

In order to fly safely long distances with safety, a reliable radio control link is required. For that purpose a Thomas Scherrer Long Range System (TSLRS) attached to a Multiplex royal EVO 9 radio is used. This LRS has been used since 2008 in the most diverse applications both civil and military with very good results.
The radio is connected to the transmission module through the PPM (Pulse Position Modulation) external port of the RC system. It operates on the UHF band (433 MHz to 440MHz), has a maximum radiated power of 2W with Frequency Hopping Spread Spectrum (FHSS). The receiver has a total of 12 output channels and has an RSSI (Receiver Signal Strength Indication) output that indicates the signal strength. It also as a PPM output that is very convenient, because it dramatically reduces the wiring between the receiver and the autopilot to just only two cables, one being the RSSI and other the PPM out.

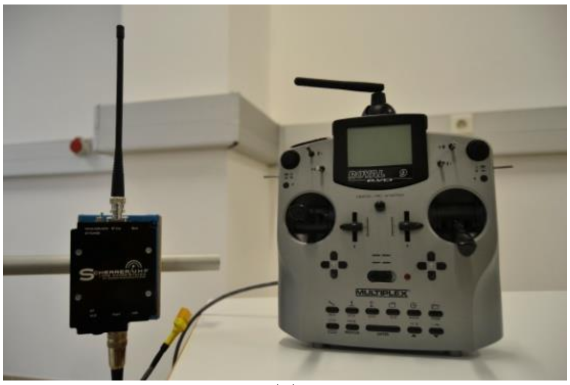

(a)

(b)

Figure 3- Complete long range radio control system showing: a) the radio controller and the LRS transmitter, and b) the LRS receiver.

In Figure 4 it is possible to observe the overall complete system. This is a totally portable system, user friendly, easy to operate with minimum knowledge of the system and it is also assembled in a short time period. Only two people are required for operating this system, one at the control of the UAV and the other monitoring the UAV flight telemetry on the computer.

Figure 4- Complete UAV System

4. Autopilot System

The autopilot system that is used on the UAV is the ArduPilot Mega 2.5 (APM 2.5) which is interfaced and controlled using the ArduPlane, an open source autopilot software. This system is capable of transforming any kind of aerial vehicle on a fully autonomous vehicle that can perform programmed missions through waypoints. In the present case, the autopilot is essentially used as a platform for acquiring all kinds of sensor data and sending this data to the telemetry ground station in order to record it and later post-process it. This system is composed by two main categories: the autopilot board and the telemetry ground station.

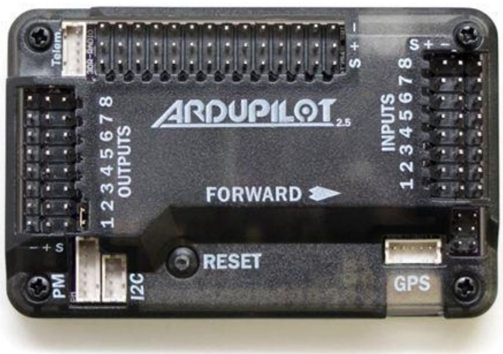

Figure 5- APM 2.5 board

4.1 Autopilot board

The autopilot board used, as described previously, is an APM 2.5. This board has several internal sensors such as 3-axis gyros, 3-axis accelerometers, a magnetometer, a GPS system and a barometric pressure sensor. With this autopilot it is possible to add other external sensors. The external sensors used on the UAV are a differential pressure sensor that is used for determining the airspeed, a voltage and current sensor that are included in the power module that also feeds the autopilot via a linear regulator and a RSSI signal coming from the receiver. This board has 8 standard RC channel inputs (PWM) but only one is used since the RC receiver is feeding the APM with a PPM signal that synthesizes all the 8 channels. The outputs are connected to all servos and the motor. The APM uses the 3DR uBlox LEA-6H GPS which is fitted on the wing, away from electromagnetic noise generated by the electrical motor and the video transmitter. The autopilot board is installed in the fuselage underneath the wing, coincident with the centre of gravity of the UAV. It is shown in Figure 5.

4.2 Telemetry ground station

The telemetry ground station is constituted by a laptop with the Ardupilot Mission Planner software and a 2.4GHz FHSS Laird Module with standard 2dBi dipole.
The Ardupilot Mission Planner is an open source autopilot software where the autopilot can be tuned and the missions can be programmed. Furthermore, all the telemetry data can be shown and stored with this application. This software was chosen because it has a good interface and it is very intuitive when configuring the autopilot.
When using the Autopilot mode, it is necessary to define waypoints and Ardupilot Mission Planner interfaces with Google Maps to facilitate waypoints positioning. The waypoints are then transferred to the APM 2.5 and the autopilot controller ensures that the UAV will strictly follow the defined waypoints coordinates. There are also other flight modes that can be triggered: Stabilize, Fly By Wire (FBW), Return To Launch (RTL) inter alia. The RTL mode is very useful because in case of video signal loss or long range radio control system failure, this mode is engaged and the UAV will automatically return to home position.

5. UAV Flight Testing

5.1 Skywalker UAV flight testing

The first step before getting airborne is to check all systems range. For that purpose two places with line of sight separated from a determined and fixed distance are chosen. Figure 6 represents the map terrain where the yellow marks represent the places chosen to position the ground station and the UAV.

Figure 6-Google earth image showing the two places chosen for range testing.

The objective of this test is to observe the variation of the RSSI signal with the distance from the GCS and the UAV and to check that all systems are working properly. The two places chosen are apart 1.1km and the observed RSSI signal was 96%. This distance is relatively short for the normal UAV operation, but it is a good starting point for evaluating possible interferences between telemetry transceiver, video transmitter and LRS receiver. At this distance the video signal received on the GCS was clear, in other words it did not had any noise. Regarding the telemetry feed, it was observed that even at half radiated power of the transceivers, the telemetry ground station was able to receive the incoming flight data. However the signal quality was mediocre. In order to increase the signal stability it was decided to use full power (125mW).

After checking the range of all systems, flight tests in manual mode are conducted. In manual mode the aircraft is trimmed to fly level without pilot compensation. After trimming the UAV, other modes beside manual are tested. The second flight mode that needs to be tested is FBW-A mode. It is in this fight mode where the gains of the autopilot PID controller are adjusted. These gains are tuned on the autopilot software Ardupilot Mission Planner. The gains tuning is an iterative process between changing the PID gains on Ardupilot Mission Planner and watching the UAV response to those changes. When the gains are well adjusted all the other flight modes that include navigation such as RTL and Auto can be tested.
At the present time, no other flight modes beside manual were tested. Further flight testing is scheduled shortly.

5.2 Olharapo UAV flight testing

All the flight tests are conducted with the purpose of determining the performance of the VSW and conventional wing. This consists on determining the lift-to-drag ratio of the vehicle as a function of airspeed for different VSW positions, from fully extended to fully retracted, and the roll control authority and energy requirements regarding actuation during a typical mission profile. All the acquired flight data is then post-processed, so that a comparison between these two wings can be made afterwrds.
The UAV airframe developed in previous works by Aerospace Sciences Department of University of Beira Interior was adapted in order to receive the VSW and to fit all the necessary systems to measure in-flight parameters and communicate them back in real time to the ground control station. An H-tail was also introduced to replace the original V-tail configuration. The H-tail configuration allows the UAV to perform safe roll manoeuvres with rudder and elevon deflections (asymmetrical deflection of elevator) without the need for aileron actuation. This can be seen as a precaution measure that guarantees roll manoeuvres in the case of VSW asymmetrical wing inadequate control authority or deployment failure. In Figure 7 it is possible to see Olharapo UAV in the two different configurations.

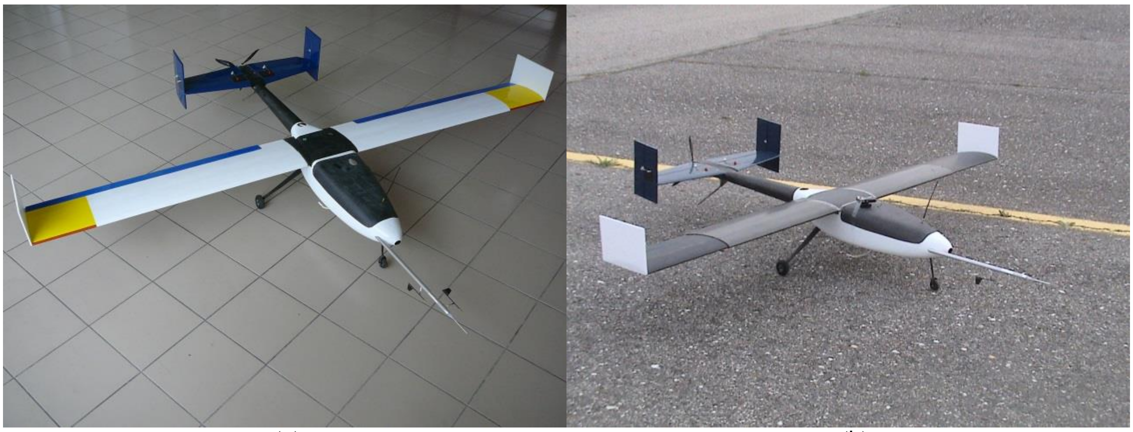

(a) (b)

Figure 7-Olharapo UAV fitted with: a) Conventional fixed wing and b) Variable-span wing

There are two main ways of determining the lift-to-drag ratio. The first consists on a straight and level flight where the UAV is flying at a given trimmed speed. In this levelled flight condition, the lift (L) equals weight (W), and the drag (D) equals thrust (T). The thrust is acquired by a load cell installed in the aircraft and connected to the motor and the weight of the UAV is previously known. With the lift and drag determined it is now possible to obtain the lift-to-drag ratio (L/D). The second way consist on a steady-state glide. In this flight condition, the only forces to vectorially balance the weight are lift (L) and drag (D) that are given by the following equations:

$$L = W * \cos(\gamma)$$
$$D = -W * \sin(\gamma)$$

where W is the known weight of the UAV and γ is glide angle provided by the autopilot. Having lift and drag determined it is now possible to calculate the lift-to-drag ratio (L/D). Both this methods require intensive test flights so that several airspeeds and flight conditions can be tested.

6. Conclusions

All work described in this paper is an intermediate step to characterize the performance with precision and simultaneously with safety of the Olharapo UAV in both configurations: fixed wing and variable-span wing. With the aim of validating all the systems related to the flight performance determination, the Skywalker UAV, used as a testbed, was outfitted with a telemetry system, a video system, an autopilot system and a long range piloting system. All these systems proved to be very reliable and definitely fulfilled all the expectations. The ground control station demonstrated to be very easy and fast to assemble and the FPV camera coped very well with direct sun light exposure. The video signal was clear during all the flight tests and no occurrence of noise was detected. Regarding the long range radio control system, it was observed that this system at the configuration of minimum radiated power has more than sufficient range for performing performance evaluating flights. The overall systems work very well together and are assembled in a matter of only 5 minutes.
The results so far obtained are encouraging because these systems showed satisfactory performance at various levels such as reliability, precision and easy operation.

7. Future work

The future work in this subject will involve two major areas. The first and more obvious is to finish the work on the Skywalker UAV. This will involve autopilot tuning to achieve fully autonomous flight. It will also be necessary to develop and refine standard test procedures to perform the steady-state glide in order to determine the glide ratio. After finishing all the test flights with Skywalker, all the systems will be transferred to Olharapo. The work that needs to be developed in Olharapo goes through adding more external sensors such as voltage and current sensors to measure the power consumption of the VSW actuation system and the load cell that needs to be installed and calibrated. The installation of the load cell will allow the determination of the glide ratio with a direct measuring of the UAV thrust. As a new way of determining the glide ratio, standard test procedures will also have to be developed.

Acknowledgements

The work presented herein has been partially funded by the European Community's Seventh Framework Programme (FP7) under the Grant Agreement 314139. The CHANGE project (Combined morphing assessment software using flight envelope data and mission based morphing prototype wing development) is a Level 1 project funded under the topic AAT.2012.1.1-2. involving 9 partners. The project started on August 1st 2012.

References

[1] Tidwell Z., Joshi S., Crossley W., and Ramakrishnan S., "Comparison of Morphing Wing Strategies Based Upon Aircraft Performance Impacts", AIAA Paper 2004-1722, *45th AIAA/ASME/ASCE/AHS/ASC Structures, Structural Dynamics and Materials Conference*, Palm Springs, California, 19-22 April, 2004.
[2] Gamboa P., Vale J., Lau F., and Suleman A., "Optimization of a Morphing Wing Based on Coupled Aerodynamic and Structural Constraints", *AIAA Journal*, Vol. 47, No. 9, September 2009, pp. 2087-2104.
[3] Neal D., Good M., Johnston C., Robertsha H., Mason W., and Inman D., "Design and Wind-Tunnel Analysis of a Fully Adaptive Aircraft Configuration", *AIAA Paper 2004-1727*, *45th AIAA/ASME/ASCE/AHS/ASC Structures, Structural Dynamics and Materials Conference*, Palm Springs, California, April 19-22, 2004.

[4] Vocke R., Kothera C., Woods B., Bubert E., Wereley N., One Dimensional Morphing Structures for Advanced Aircraft, Recent Advances in Aircraft Technology, Dr. Ramesh Agarwal (Ed.), ISBN: 978-953-51-0150-5, InTech, DOI: 10.5772/37333. http://www.intechopen.com/books/recent-advances-in-aircraft-technology/onedimensional-morphing-structures-for-advanced-aircraft (03/08/2013)
[5] Sunil C. Patel, Manoranjan Majji, Bong Su Koh, John L. Junkins, Othon K. Rediniotis., "Morphing Wing: A Demonstration of Aero Servo Elastic Distributed Sensing and Control", Tiims USRG Report, August 2005
[6] Elzey D., Sofla A., Wadley H., "A bio-inspired, high-authority actuator for shape morphing Structures", Smart Structures and Materials 2003: Active Materials: Behavior and Mechanics. Edited by Lagoudas, Dimitris C. Proceedings of the SPIE, Volume 5053, pp. 92-100 (2003)
[7] Blondeau J., and Pines D., "Pneumatic Morphing Aspect Ratio Wing", *AIAA Paper 2004-1808, 45th AIAA/ASME/ASCE/AHS/ASC Structures, Structural Dynamics and Materials Conference*, Palm Springs, California, April 19-22, 2004.
[8] Cadogan D., Graham W., and Smith T., "Inflatable and Rigidizable Wings for Unmanned Aerial Vehicles," *AIAA Paper 2003-6630, 2nd AIAA "Unmanned Unlimited" Systems*, San Diego, California, September 2003.
[9] Bowman J., Sanders B., and Cannon B., "Development of Next Generation Morphing Aircraft Structures", *AIAA Paper 2007-1730, 48th AIAA/ASME/ASCE/AHS/ASC Structures, Structural Dynamics, and Materials Conference*, Honolulu, Hawaii, 23-26 April 2007.
[10] Flanagan J.S., Strutzenberg R.C., Myers R.B., and Rodrian J.E., "Development and Flight Testing of a Morphing Aircraft, the NextGen MFX-1", *AIAA Paper 2007-1707, 48th AIAA/ASME/ASCE/AHS/ASC Structures, Structural Dynamics, and Materials Conference*, Honolulu, Hawaii, 23-26 April 2007.
[11] Babarino S., Bilgen O., Ajaj R.M., Friswell M.I., and Inman D.J., "A Review of Morphing Aircraft", *Journal of Intelligent Material Systems and Structures*, Volume 22, June 2011, pp. 823-877.
[12] Secanell M, Suleman A, and Gamboa P, "Design of a Morphing Airfoil Using Aerodynamic Shape Optimization", *AIAA Journal*, Volume 44, Number 7, pp. 1550-1562.
[13] Marques M., Gamboa P., and Andrade E., "Design of a Variable Camber Flap for Minimum Drag and Improved Energy Efficiency", *50th AIAA/ASME/ASCE/AHS/ASC Structures, Structural Dynamics, and Materials Conferences*, Palm Springs, California, 4-7 May, 2009.
[14] Mestrinho J., Gamboa P., and Santos P., "Design Optimization of a Variable-Span Morphing Wing for a Small UAV", *52th AIAA/ASME/ASCE/AHS/ASC Structures, Structural Dynamics and Materials Conference*, Denver, Colorado, 4-7 April, 2011.
[15] Felício J., Santos P., Gamboa P., and Silvestre M., "Evaluation of a Variable-Span Morphing Wing for a Small UAV", *52th AIAA/ASME/ASCE/AHS/ASC Structures, Structural Dynamics and Materials Conference*, Denver, Colorado, 4-7 April, 2011.
[16] Grass F., Lawrence D., Calhoun S., Campbell J., "Instrumentation of UAV for 6-DOF Modeling". Proceedings of quarterly review of the NASA/FAA joint university, Program for Air Trasportation Reseacrh, Athens Ohio, USA, 14 June, 2002.